Biomedical Signal Processing and Control 5 (2010) 53–58

Contents lists available at ScienceDirect

Biomedical Signal Processing and Control

journal homepage: www.elsevier.com/locate/bspc

Screening of knee-joint vibroarthrographic signals using probability density functions estimated with Parzen windows

Rangaraj M. Rangayyan [a,*], Yunfeng Wu [b]

[a] Department of Electrical and Computer Engineering, Schulich School of Engineering, University of Calgary, Calgary, AB, Canada T2N 1N4
[b] School of Information Engineering, Beijing University of Posts and Telecommunications, 10 Xi Tu Cheng Road, Haidian District, Beijing 100876, China

ARTICLE INFO

Article history:
Received 6 January 2009
Received in revised form 25 March 2009
Accepted 30 March 2009
Available online 5 May 2009

Keywords:
Vibroarthrography
Knee-joint sounds
Probability density function
Parzen-window
Kullback-Leibler distance
Modeling

ABSTRACT

Pathological conditions of knee joints have been observed to cause changes in the characteristics of vibroarthrographic (VAG) signals. Several studies have proposed many parameters for the analysis and classification of VAG signals; however, no statistical modeling methods have been explored to analyze the distinctions in the probability density functions (PDFs) between normal and abnormal VAG signals. In the present work, models of PDFs were derived using the Parzen-window approach to represent the statistical characteristics of normal and abnormal VAG signals. The Kullback-Leibler distance was computed between the PDF of the signal to be classified and the PDF models for normal and abnormal VAG signals. Additional statistical measures, including the mean, standard deviation, coefficient of variation, skewness, kurtosis, and entropy, were also derived from the PDFs obtained. An overall classification accuracy of 77.53%, sensitivity of 71.05%, and specificity of 82.35% were obtained with a database of 89 VAG signals using a neural network with radial basis functions with the leave-one-out procedure for cross validation. The screening efficiency was derived to be 0.8322, in terms of the area under the receiver operating characteristics curve.

1. Introduction

Abnormal conditions in the knee joint are expected to lead to variations in the vibroarthrographic (VAG) signal, which represents the sound or vibration emitted from the joint during flexion or extension [1]. Digital signal processing and pattern classification techniques have been applied to VAG signals to derive features that can characterize the state of the articular cartilage surfaces, and assist in noninvasive detection and diagnosis of knee-joint pathology [1–11]. Screening for knee-joint pathology using VAG signals could reduce or obviate the need for diagnostic surgery. Such methods could also find application in monitoring the functional integrity or deterioration over time of natural as well as prosthetic joints [8].

A significant portion of patients who undergo arthroscopy have been observed to be free of abnormalities of the joint [12]. Imaging techniques such as computed tomography and magnetic resonance imaging (MRI) have limited application in the diagnosis of knee-joint pathology, in particular in repeated investigation or monitoring. Orthopedic surgeons and related specialists are interested in the development of methods for noninvasive screening of patients prior to the recommendation of procedures such as arthroscopic examination. Meniscal tears usually cannot be observed in X-ray examinations. Often, MRI of an injured knee is performed to investigate potential meniscal tears; arthroscopy is performed if MRI indicates a meniscal tear. MRI is expensive and not easily accessible; a noninvasive quantitative assessment technique could assist in such a situation. To address this need, we are developing screening methods and systems for use in the clinic of a physician or an orthopedic specialist [1,13]. In the present work, we investigate the use of statistical modeling of the probability density functions (PDFs) of the signals and parameters derived thereof to characterize the distinction between normal and abnormal VAG signals [14].

2. Materials and methods

2.1. VAG signal data acquisition

The signals used in the present work were acquired in previous related studies [6,15]. Each subject sat on a rigid table in a relaxed position with the leg being tested freely suspended in air. The VAG signal was recorded by placing an accelerometer (model 3115a, Dytran, Chatsworth, CA) at the mid-patella position of the knee as the subject swung the leg over an approximate angle range of 135° (approximately full flexion) to 0° (full extension) and back to 135°

* Corresponding author. Tel.: +1 403 220 6745; fax: +1 403 282 6855.
E-mail address: ranga@ucalgary.ca (R.M. Rangayyan).

1746-8094/$ – see front matter © 2009 Elsevier Ltd. All rights reserved.
doi:10.1016/j.bspc.2009.03.008

in 4 s [6,15]. The first half (approximately) of each VAG signal corresponds to extension, and the second half to flexion of the leg. Auscultation of the knee joint using a stethoscope was also performed, and a qualitative description of sound intensity and type was recorded, along with their relationship to joint angle. Informed consent was obtained from each subject. The experimental protocol was approved by the Conjoint Health Research Ethics Board of the University of Calgary.

The VAG signal was prefiltered (10 Hz to 1 kHz) and amplified before digitizing at a sampling rate of 2 kHz. Each signal was normalized to the amplitude range $[0, 1]$. Fig. 1 shows examples of normal and abnormal VAG signals. The abnormal signal exhibits a higher degree of overall variation, activity, or complexity than the normal signal.

The database used in the present study consists of 89 signals, with 51 from normal volunteers and 38 from subjects with knee-joint pathology. The normals were established by clinical examination and history. The abnormal signals were collected from symptomatic patients scheduled to undergo arthroscopy independent of the VAG studies. The abnormal signals include chondromalacia of different grades at the patella, meniscal tear, tibial chondromalacia, and anterior cruciate ligament injuries, as confirmed during arthroscopic examination. The dataset available is not adequate to permit classification of the signals into various types or stages of pathology. The present study is aimed at screening only, that is, normal versus abnormal classification.

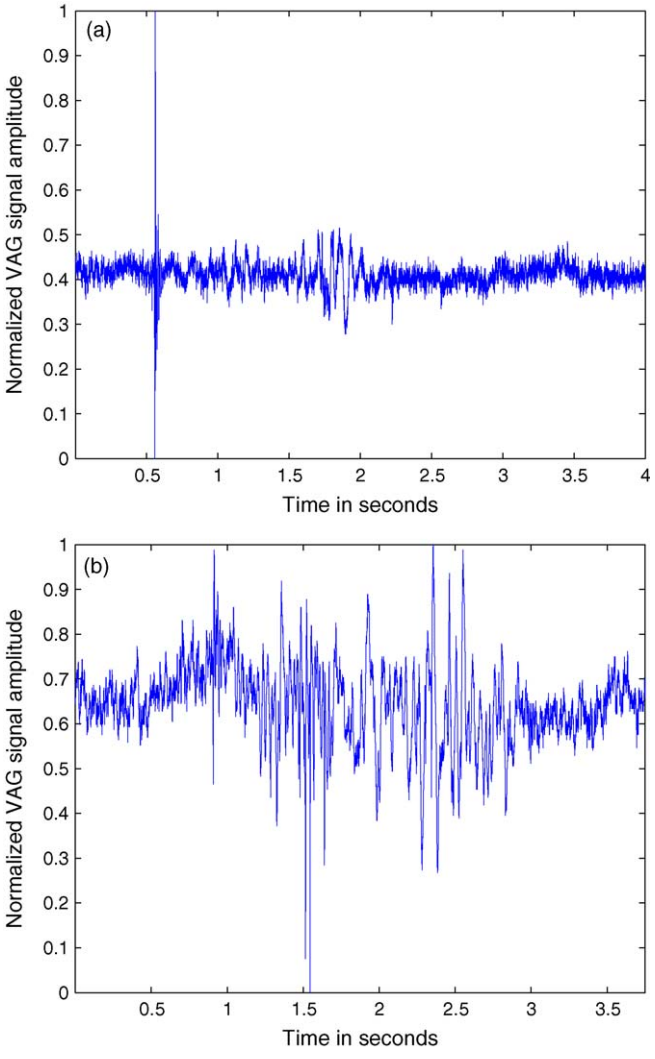

Fig. 1. VAG signal examples of a: (a) normal subject; (b) patient with knee-joint pathology. The amplitude has been normalized to the range $[0, 1]$.

As compared to previous related studies [5–7], the dataset used in the present study lacks one abnormal VAG signal due to corruption of the data. The present study uses the same dataset as that used in a few recent studies [1,10,11,13,14].

2.2. Modeling the PDFs with the Parzen-window method

In our previous studies, VAG signals related to various types of knee-joint pathology have been observed to possess a larger extent of variability over the duration of a swing cycle of the leg than normal VAG signals [1,10,11,13–16]. To characterize this nature of VAG signals, Moussavi et al. [16] used the variance of the means of the segments of a given VAG signal; the signals were segmented adaptively using a recursive least squares algorithm. We have recently explored the use of statistical parameters such as the form factor (based upon the variance of the first and second derivatives of the given signal), skewness, kurtosis, and entropy [1] as well as an adaptive turns count and the variance of the mean-squared value [13] for screening of VAG signals. Other methods that have been proposed for the analysis of VAG signals include autoregressive modeling [5,6], cepstral coefficients [6], time-frequency distributions [7], and wavelet packet decomposition [10]; see Rangayyan and Wu [1] for a recent review. However, the methods mentioned above do not characterize the complete statistical nature or probabilistic distributions of the signals. In the present work, we derive models of the PDFs, using the Parzen-window approach [17,18], to represent the basic statistical characteristics of normal and abnormal VAG signals [14].

To obtain the PDF models, a histogram is computed by combining all of the normal signals into one group. The histogram is denoted by $h_n(x_l)$, with x_l, $l = 0, 1, 2, \ldots, L-1$, representing the L bins used to represent the range of the values of the signal x. In the present work, we use $L = 100$ bins to represent the normalized range of $[0, 1]$ for the VAG signal values. Experiments were conducted with a number of values for L. A large value for L would lead to several bins with negligible or zero counts, whereas a small value would lead to diminished differences between the histograms for normal and abnormal signals. The value of $L = 100$ was selected based on an analysis of the results with several values of L. Similarly, a histogram $h_a(x_l)$ is obtained by pooling together all of the abnormal signals. Each histogram is normalized by dividing by the total number of samples in the population, so that the area under the normalized histogram is unity. A Gaussian fit is then obtained for each of the two histograms obtained as above, denoted as $g_n(x_l)$ and $g_a(x_l)$.

The Parzen-window approach to obtain a nonparametric estimate of the PDF from a collection of samples is then applied as follows [17,18]. Consider the situation where we have available a set of independent samples, $Z = \{z_1, z_2, \ldots, z_K\}$, with an unknown underlying PDF $p(z)$. A nonparametric estimate of $p(z)$ from Z is provided by the function [17,18]

$$\hat{p}(z) = \frac{1}{K}\sum_{k=1}^{K}\kappa(z - z_k), \tag{1}$$

where κ is a window or kernel function that integrates to unity. In the present work, we use

$$\kappa(z - z_k) = \frac{1}{\sigma_P\sqrt{2\pi}}\exp\left[-\frac{(z - z_k)^2}{2\sigma_P^2}\right]. \tag{2}$$

The Parzen-window PDF is estimated using the quantized values of the signals, x_l, $l = 0, 1, 2, \ldots, L-1$, with $L = 100$ levels, in the normalized range $[0, 1]$. Experiments were conducted with the

value of the parameter σ_P in Eq. (2) varying over the range $[0.01, 0.1]$ in steps of 0.01; in the present work, the value is set equal to 0.04.

2.3. The Kullback-Leibler distance

The Kullback-Leibler distance (KLD) between two PDFs $p_1(x_l)$ and $p_2(x_l)$ is defined as [17]

$$\mathrm{KLD}(p_1, p_2) = \sum_{l=0}^{L-1} p_2(x_l) \ln\left[\frac{p_2(x_l)}{p_1(x_l)}\right]. \quad (3)$$

In the present work, we compute the KLD between the PDF estimated for the signal to be classified and the PDF models for the normal and abnormal VAG signals. In obtaining the PDF models for the normal and abnormal signals with the limited dataset available, the leave-one-out (LOO) method is used: the signal to be classified is left out of the procedure to obtain the Parzen-window model for the corresponding class. In this manner, the signal being tested does not contribute to the training process.

2.4. Statistics of the VAG signals from the PDFs

One of our previous studies [1] has demonstrated that statistical measures, including skewness, kurtosis, and entropy [19,20], can provide good performance in discriminating between normal and abnormal VAG signals. The measures are based upon the moments of the PDF of the given signal, denoted by $p_x(x_l)$, with $x_l, l = 0, 1, 2, \ldots, L-1$, representing the L bins used to represent the range of the values of the signal x. In the present work, we have set $L = 100$. The k th central moment of the PDF $p_x(x_l)$ is defined as

$$m_k = \sum_{l=0}^{L-1} (x_l - \mu)^k \, p_x(x_l), \quad (4)$$

where μ is the mean value, given by

$$\mu = \sum_{l=0}^{L-1} x_l \, p_x(x_l). \quad (5)$$

The variance is given by

$$\sigma^2 = m_2 = \sum_{l=0}^{L-1} (x_l - \mu)^2 \, p_x(x_l). \quad (6)$$

The ratio of the standard deviation to the mean, known as the coefficient of variation (CV), was also computed in the present work:

$$\mathrm{CV} = \frac{\sigma}{\mu}. \quad (7)$$

The normalized third and fourth moments, known as the skewness (S) and kurtosis (K), respectively, are defined as

$$S = \frac{m_3}{(m_2)^{3/2}}, \quad (8)$$

and

$$K = \frac{m_4}{(m_2)^2}. \quad (9)$$

Skewness is related to asymmetry of the PDF. Kurtosis is related to the presence of a long tail in the PDF; it also represents the "peakedness" of the PDF.

Entropy is a commonly used measure to represent the nature and spread of a PDF, and is defined as

$$H = -\sum_{l=0}^{L-1} p_x(x_l) \log_2[p_x(x_l)]. \quad (10)$$

The entropy is maximum for a uniformly distributed PDF, and has lower values for PDFs with narrow ranges of significant probability values.

The parameters listed above were derived from the Gaussian as well as Parzen-window PDFs of the VAG signals.

2.5. Feature selection and screening of VAG signals

In order to derive a receiver operating characteristics (ROC) curve, the KLDs of the PDF of the signal to be classified to the normal and abnormal PDF models were combined into a single discriminant feature by taking their difference; this value shall be referred to as dKLD. An ROC curve was generated by using the software tool ROCKIT provided by the University of Chicago [21,22]. The area (A_z) under the ROC curve was derived to serve as a summary measure of the overall classification performance. The same procedure was applied to each of the statistical parameters defined in Section 2.4, namely μ, σ, CV, S, K, and H, individually. The features were analyzed for their individual discriminant capability using their A_z values. The features were also analyzed for the statistical significance of the difference between the normal and abnormal categories by applying the t-test and deriving the p-values [23].

Pattern classification experiments were conducted by using neural networks with radial basis functions (RBF) [24], using different sets of selected features and the LOO procedure for cross validation [17]. An RBF network (RBFN) with a feed-forward hidden layer applies a nonlinear transformation from the input space to a high-dimensional hidden space, and then produces separable responses through a linear output transformation; see Rangayyan and Wu [1,13] for details and illustrations of the RBFN. The result of the RBFN may be used to classify the signals by applying a threshold, or a sliding threshold may be applied to generate an ROC curve. For comparative analysis, classification experiments were also conducted using classical method of Fisher linear discriminant analysis (FLDA) [17].

The details of the RBFN used in the present work are as follows: The input layer included up to seven nodes to accept various sets of features extracted from each VAG signal. The spread parameter was varied over the range $[1, 6]$, and the number of hidden nodes was varied over the range $[1, 30]$. The parameters of the final RBFN selected for the illustration of results in the present paper are number of hidden neurons = 29, and the spread parameter = 5. The resulting output values were used to derive ROC curves and the associated A_z values using ROCKIT.

3. Results

Fig. 2 shows the Parzen-window estimates of the PDFs of the normal and abnormal VAG signals shown in Fig. 1. Fig. 3 shows the Parzen-window estimates of the PDFs of the 51 normal and 38 abnormal VAG signals in the database used. The amplitude has been normalized to the range $[0, 1]$. Also shown are the normalized histograms and the Gaussian fits for each case.

The following observations were made from the PDFs of the normal and abnormal VAG signals:

- In general, the Parzen-window PDFs are closer to the normalized histograms of the VAG signals than the corresponding Gaussian

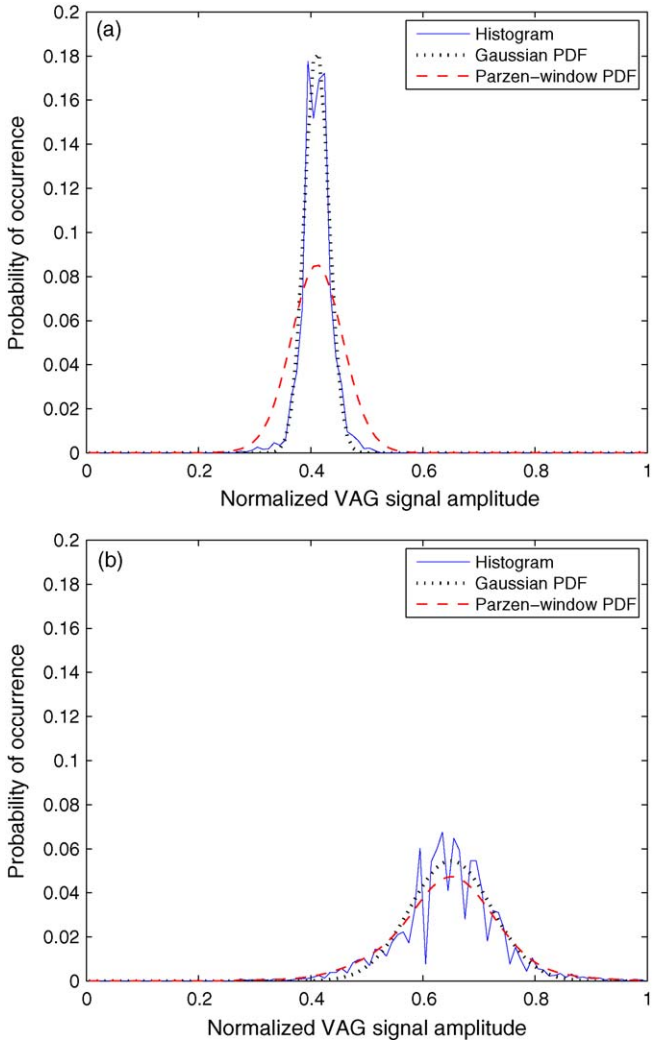

Fig. 2. Nonparametric Parzen-window estimates of the PDFs of the VAG signals in Fig. 1: (a) normal subject; (b) patient with knee-joint pathology. The amplitude has been normalized to the range $[0, 1]$. Also shown are the normalized histogram and the Gaussian fit for each case. The parameters of the Gaussian fit are (a) mean = 0.4107, standard deviation = 0.0216; (b) mean = 0.6499, standard deviation = 0.0730.

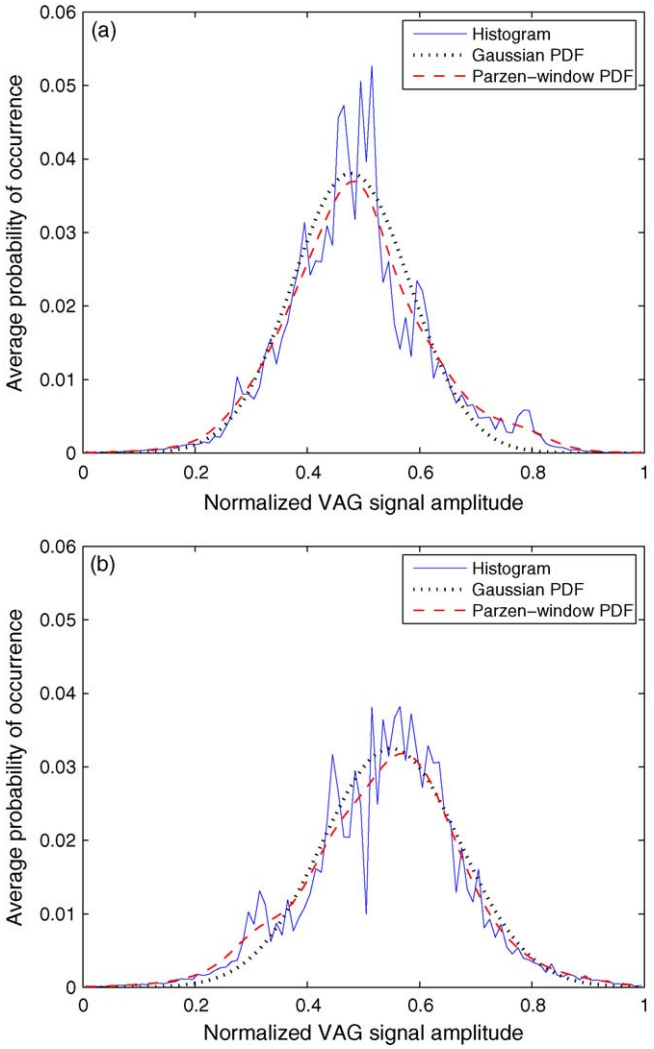

Fig. 3. Nonparametric Parzen-window estimates of the PDFs of VAG signals: (a) derived from VAG signals of 51 normal volunteers; (b) derived from VAG signals of 38 subjects with knee-joint pathology. The amplitude has been normalized to the range $[0, 1]$. Also shown are the normalized histogram and the Gaussian fit for each case. The parameters of the Gaussian fit are (a) mean = 0.4778, standard deviation = 0.1047; (b) mean = 0.5495, standard deviation = 0.1227.

models. The closeness of the fit depends upon the value of σ_P used: the smaller the value of σ_P, the better the fit. However, a larger value of σ_P is desirable to obtain smooth model PDFs that do not include irrelevant details of the histograms of the signals. A balance needs to be achieved between these two requirements. After experimenting with several values of σ_P in the range $[0.01, 0.1]$, the value of $\sigma_P = 0.04$ was chosen in the present work.

- The PDF models for the abnormal signals indicate that the abnormal signals have higher probabilities of occurrence of higher values within the normalized range $[0, 1]$.
- Based on the differences between the PDF models for the normal and abnormal signals, it should be possible to classify VAG signals using parameters derived from their PDFs.
- The differences apparent between the PDF models suggest the existence of different underlying signal-generation processes or statistical models for normal and abnormal VAG signals.

Using only the dKLD feature obtained with the Parzen-window models with the FLDA and LOO methods, a normal-versus-abnormal classification accuracy of 73.03% was obtained with the database of 89 VAG signals used. The sensitivity and specificity of classification (screening) were calculated to be 68.42% and 76.47%, respectively. The screening efficiency was found to be $A_z = 0.6987$ with a standard error (SE) of 0.0558. The use of dKLD with the Gaussian models resulted in a poorer performance, with overall accuracy of 69.66%, sensitivity of 57.89%, specificity of 78.43%, and $A_z = 0.6748$ (with SE = 0.0568). Note that the Gaussian model does not facilitate the characterization of asymmetric or skewed PDFs.

Pattern classification using each of the statistical parameters derived from the PDF models individually (as defined in Section 2.4, namely μ, σ, CV, S, K, and H) did not yield results better than the above; the single exception was μ obtained from the Parzen-window models, which led to an overall accuracy of 69.66%, sensitivity of 65.79%, specificity of 72.55%, and $A_z = 0.7107$ (with SE = 0.0546). Selected results are summarized in Table 1.

Based upon their individual performance in terms of A_z and p-values, several combinations of the proposed features were tested using the FLDA and RBFN methods with the LOO procedure. The best classification performance was provided by the feature set {dKLD, K, H, μ, σ}, with an overall accuracy = 77.53%, sensitivity = 71.05%, specificity = 82.35%, and $A_z = 0.8322$ (SE = 0.0429) using the RBFN with LOO.

Table 1
Statistical significance of separability (p-value) and classification performance (area A_z under the ROC curve and the associated standard error, SE) of the features used for the screening of VAG signals.

Feature/classifier	p-value	A_z	SE
dKLD	0.0131	0.6987	0.0558
μ	0.0080	0.7107	0.0546
σ	0.0201	0.6155	0.0589
CV	0.2262	0.5458	0.0607
S	0.2070	0.6694	0.0566
K	0.0201	0.6155	0.0589
H	0.0299	0.6138	0.0590
FLDA/LOO using all 7 features	N/A	0.6360	0.0596
FLDA/LOO using {dKLD, μ}	N/A	0.6360	0.0596
FLDA/LOO using {dKLD, K, H, μ, σ}	N/A	0.6360	0.0596
RBFN/LOO using all 7 features	N/A	0.6278	0.0589
RBFN/LOO using {dKLD, μ}	N/A	0.7450	0.0525
RBFN/LOO using {dKLD, K, H, μ, σ}	N/A	0.8322	0.0429

All VAG signal features were obtained from the Parzen-window PDFs with $\sigma_P = 0.04$. dKLD: difference between the Kullback-Leibler distances to the normal and abnormal PDFs. μ: mean. σ: standard deviation. CV: coefficient of variation. S: skewness. K: kurtosis. H: entropy. FLDA: Fisher linear discriminant analysis. LOO: Leave-one-out cross validation. RBFN: Neural network with radial basis functions. N/A: not applicable.

4. Discussion and conclusion

In comparison with the results reported in previous studies on the analysis of VAG signals with the same dataset as in the present study (except for the loss of one signal), the results obtained in the present study are important in that the proposed parameters, derived from the VAG signals with no segmentation and no additional clinical information, have provided screening accuracies comparable to or better than those obtained with more sophisticated methods, such as autoregressive modeling (68.9% and 70%) [5,6], cepstral coefficients (75.6%) [6], time-frequency distributions (68.9%) [7], and wavelet packet decomposition (79.8%) [10]. In our recent related studies using the same dataset as in the present study, the best screening performance obtained was $A_z = 0.8172$ with form factor, skewness, kurtosis, and entropy [1], and $A_z = 0.9174$ with an adaptive turns count computed for flexion and extension separately [13]. The present work has yielded a comparable performance with $A_z = 0.8322$.

The RBF network parameters (the number of hidden neurons and the spread) were fixed in the LOO tests. The weights and bias of the RBFN in each LOO trial were obtained with the orthogonal least-squares (OLS) method [25]. The LOO tests provide an indication of the generalization capability of the RBFN classifier with the proposed features. In a practical application, a larger training database than that used in the present work would be required to design a single robust RBFN classifier, which would be expected to perform well with new VAG signals of the nature represented in the training database.

The proposed method has demonstrated good potential for use in noninvasive screening for articular cartilage pathology. The method obviates the need for segmentation and derivation of sophisticated parameters requiring significant computational effort, and could lead to a practical approach for the analysis of VAG signals. Although the overall accuracy of 77.53% achieved in the present study indicates the potential of the proposed methods and represents a significant step forward, a higher accuracy would be essential before clinical application of the methods. A limitation of the proposed modeling approach is that the nonstationary nature of the VAG signals is not addressed. Further work is required on feature selection and application of advanced pattern classification methods to the proposed features.

Our aim is to develop a simple screening tool for use in the clinic of a physician or an orthopedic specialist. The proposed method could be easily implemented on a digital signal processor chip that could be located in a stand-alone device or incorporated into a basic computer. Given the simple nature of the signal acquisition and analysis methods, the assessment of the knee joints of a subject could be performed in the office of a physician or outdoors in a few minutes. Improved selection of patients for further clinical or surgical procedures, such as arthroscopy, could reduce the associated risks to the patient and costs.

Acknowledgments

This work was supported by the Doctoral Program Foundation of the Ministry of Education of China under Grant No. 20060013007 awarded to Y.F. Wu, and by the University of Calgary in the form of a "University Professorship" awarded to R.M. Rangayyan. R.M. Rangayyan is a Visiting Professor at the Beijing University of Posts and Telecommunications. We thank Yachao Zhou for assistance in this work.

References

[1] R.M. Rangayyan, Y.F. Wu, Screening of knee-joint vibroarthrographic signals using statistical parameters and radial basis functions, Medical & Biological Engineering & Computing 46 (3) (2008) 223–232.
[2] M.L. Chu, I.A. Gradisar, L.D. Zavodney, Possible clinical application of a noninvasive monitoring technique of cartilage damage in pathological knee joints, Journal of Clinical Engineering 3 (1) (1978) 19–27.
[3] G.F. McCoy, J.D. McCrea, D.E. Beverland, W.G. Kernohan, R.A.B. Mollan, Vibration arthrography as a diagnostic aid in diseases of the knee, The Journal of Bone and Joint Surgery 69-B (2) (1987) 288–293.
[4] N.P. Reddy, B.M. Rothschild, M. Mandal, V. Gupta, S. Suryanarayanan, Noninvasive acceleration measurements to characterize knee arthritis and chondromalacia, Annals of Biomedical Engineering 23 (1995) 78–84.
[5] S. Krishnan, R.M. Rangayyan, G.D. Bell, C.B. Frank, K.O. Ladly, Adaptive filtering, modelling, and classification of knee joint vibroarthrographic signals for non-invasive diagnosis of articular cartilage pathology, Medical & Biological Engineering & Computing 35 (Nov. 1997) 677–684.
[6] R.M. Rangayyan, S. Krishnan, G.D. Bell, C.B. Frank, K.O. Ladly, Parametric representation and screening of knee joint vibroarthrographic signals, IEEE Transactions on Biomedical Engineering 44 (11) (Nov 1997) 1068–1074.
[7] S. Krishnan, R.M. Rangayyan, G.D. Bell, C.B. Frank, Adaptive time-frequency analysis of knee joint vibroarthrographic signals for noninvasive screening of articular cartilage pathology, IEEE Transactions on Biomedical Engineering 47 (6) (June 2000) 773–783.
[8] C.-C. Jiang, J.-H. Lee, T.-T. Yuan, Vibration arthrometry in the patients with failed total knee replacement, IEEE Transactions on Biomedical Engineering 47 (2) (Feb 2000) 218–227.
[9] N.P. Reddy, B.M. Rothschild, E. Verrall, A. Joshi, Noninvasive measurement of acceleration at the knee joint in patients with rheumatoid arthritis and spondyloarthropathy of the knee, Annals of Biomedical Engineering 29 (12) (2001) 1106–1111.
[10] K. Umapathy, S. Krishnan, Modified local discriminant bases algorithm and its application in analysis of human knee joint vibration signals, IEEE Transactions on Biomedical Engineering 53 (3) (March 2006) 517–523.
[11] T. Mu, A.K. Nandi, R.M. Rangayyan, Screening of knee-joint vibroarthrographic signals using the strict 2-surface proximal classifier and genetic algorithm, Computers in Biology and Medicine 38 (10) (2008) 1103–1111.
[12] F. Lund, B.E. Nilsson, Arthroscopy of the patello-femoral joint, Acta Orthopaedica Scandinavica 51 (1980) 297–302.
[13] R.M. Rangayyan, Y.F. Wu, Analysis of vibroarthrographic signals with features related to signal variability and radial basis functions, Annals of Biomedical Engineering 37 (1) (2009) 156–163.
[14] R.M. Rangayyan, Y.F. Wu, Modeling and classification of knee-joint vibroarthrographic signals using probability density functions estimated with Parzen windows, in: Proc. 30th Annual International Conference of the IEEE Engineering in Medicine and Biology Society, IEEE, Vancouver, BC, Canada, August 2008 , pp. 2099–2102.
[15] K.O. Ladly, C.B. Frank, G.D. Bell, Y.T. Zhang, R.M. Rangayyan, The effect of external loads and cyclic loading on normal patellofemoral joint signals, Special Issue on Biomedical Engineering, Defence Science Journal (India) 43 (July 1993) 201–210.
[16] Z.M.K. Moussavi, R.M. Rangayyan, G.D. Bell, C.B. Frank, K.O. Ladly, Y.T. Zhang, Screening of vibroarthrographic signals via adaptive segmentation and linear prediction modeling, IEEE Transactions on Biomedical Engineering 43 (1) (1996) 15–23.

[17] R.O. Duda, P.E. Hart, D.G. Stork, Pattern Classification, second ed., Wiley, New York, NY, 2001.
[18] K. Fukunaga, Introduction to Statistical Pattern Recognition, second ed., Academic Press, Inc., San Diego, CA, 1990.
[19] J.P. Marques de Sá, Applied Statistics using SPSS, STATISTICA, and MATLAB, Springer, Berlin, Germany, 2003.
[20] R.M. Rangayyan, Biomedical Signal Analysis—A Case-Study Approach, IEEE and Wiley, New York, NY, 2002.
[21] C.E. Metz, L. Pesce, Readings in ROC Analysis, with Emphasis on Medical Applications; available at www.radiology.uchicago.edu/krl/KRL_ROC/ROC_analysis_by_topic4.htm. University of Chicago, Chicago, IL, 2006.
[22] C.E. Metz, Basic principles of ROC analysis, Seminars in Nuclear Medicine VIII (4) (1978) 283–298.
[23] J.H. Ware, F. Mosteller, F. Delgado, C. Donnelly, J.A. Ingelfinger, P values, in: J.C. Bailar, F. Mosteller, III (Eds.), Medical Uses of Statistics, second ed., NEJM Books, Boston, MA, 1992, pp. 181–200.
[24] S. Haykin, Neural Networks: A Comprehensive Foundation, second ed., Prentice-Hall PTR, Englewood Cliffs, NJ, 2002.
[25] S. Chen, C.F.N. Cowan, P.M. Grant, Orthogonal least squares learning algorithm for radial basis function networks, IEEE Transactions on Neural Networks 2 (2) (1991) 302–309.